https://jksus.org

ScientificScholar®
Knowledge is power
Publisher of Scientific Journals

Journal of King Saud University – Science

2025 37 (10) 11852025

Research Article

Unveiling comparative bioactivities of Kratom leaf extracts obtained via maceration and ultrasonic techniques: Antioxidant, antimicrobial, and antibiofilm effects with molecular docking of Q-ToF-LCMS identified compounds and ADMET prediction

Taslima Begum[a], Mohd Hafiz Arzmi[b], ABM Helal Uddin[a], Mohd Salleh Rofiee[c], Syed Adnan Ali Shah[d], Humaira Parveen[e], Sayeed Mukhtar[e], Qamar Uddin Ahmed[a,*]

[a]*Drug Discovery and Synthetic Chemistry Research Group, Department of Pharmaceutical Chemistry, Kulliyyah of Pharmacy, International Islamic University Malaysia, 25200 Kuantan, Pahang, Malaysia*
[b]*Department of Fundamental Dental and Medical Sciences, Kulliyyah of Dentistry, International Islamic University Malaysia, Jalan Istana, Kuantan, 25200, Pahang, Malaysia*
[c]*Integrative Pharmacogenomics Institute (iPROMISE), University Teknologi MARA, Cawangan Selangor Kampus Puncak Alam, Bandar Puncak Alam, 42300 Puncak Alam, Selangor, Malaysia*
[d]*Faculty of Pharmacy, Atta-ur-Rahman Institute for Natural Product Discovery (AuRIns), Universiti Teknologi MARA Cawangan Selangor Kampus Puncak Alam, Bandar Puncak Alam, 42300 Puncak Alam, Selangor, Malaysia*
[e]*Organic and Medicinal Chemistry Research Lab., Department of Chemistry, Faculty of Science, University of Tabuk, Tabuk-71491, Kingdom of Saudi Arabia*

ARTICLE INFO

Keywords:
ADMET
Antimicrobial
Antioxidant
In silico
In vitro
Kratom
Q-ToF-LCMS

ABSTRACT

Traditional medicinal practices across Southeast Asia, particularly in Thailand and Malaysia, have long utilized Kratom *(Mitragyna speciosa)* leaves for the treatment of various health conditions. However, the medicinal potential of this plant has not been properly examined. Hence, this research study was performed to explore the antioxidant, antimicrobial, and antibiofilm properties of Kratom leaf extracts, along with the identification of biologically active phytochemical components via quadrupole time-of-flight liquid chromatography-mass spectrometry (Q-ToF-LCMS) and *in silico* approaches to assess their potential as new antibacterial agents. Accordingly, 12 leaf extracts were prepared and categorized into three distinct groups based on extraction techniques: maceration, ultrasound-assisted extraction (UAE), and fractionation. Each extract was subjected to phytochemical screening, including assessments of total phenolic content (TPC), total flavonoid content (TFC), and antioxidant activity via DPPH radical scavenging and Ferric Reducing Antioxidant Power Assay (FRAP) reduction assays. In addition, antibacterial and antibiofilm activities were evaluated using disc diffusion, broth microdilution, and biofilm inhibition assays against *Escherichia coli*, *Streptococcus mutans,* and *Staphylococcus aureus*. Ultimately, 100% methanol extracts, obtained through both maceration and ultrasonic extraction, exhibited the highest antioxidant activity across all tested parameters. Specifically: maceration (100% Methanol M) (TPC: 257.46 ± 1.32 mg GAE/g extract; TFC: 50.75 ± 0.24 mg QE/g extract; FRAP: 2103.46 ± 5.67 mg AAE/g extract, DPPH IC_{50}: 7.94 ± 0.12 µg/mL), and ultrasonic extraction (100% Methanol U) (TPC: 340.99 ± 2.38 mg GAE/g extract; TFC: 62.95± 0.77 mg QE/g extract; FRAP: 2365.99 ± 3.39 mg AAE/g extract, DPPH IC_{50}: 7.57 ± 0.24 µg/mL). Among the fractions derived from 100% methanol maceration, the ethyl acetate fraction demonstrated superior antioxidant activity compared to the corresponding alkaloid fraction, with the following values: (TPC: 337.00 ± 19.60 mg GAE/g extract; TFC: 57.72 ± 3.79 mg QE/g extract; FRAP: 2981.70 ± 40.6 mg AAE/g extract, DPPH IC_{50}: 15.03 ± 0.54 µg/mL). The ethyl acetate fraction exhibited the highest activity with MICs of *S. aureus* (1.25 mg/mL) and *S. mutans* (2.5 mg/mL). Compounds identified through Q-ToF LC-MS analysis demonstrated favorable molecular interactions and strong binding affinities with the target protein of *S. aureus* (PDB ID: 3U2D) as revealed by molecular docking studies. Finally, 6-hydroxyluteolin 5-rhamnoside, kaempferol 3-(6"-p-coumarylglucoside)-7-glucoside, 6-hydroxyluteoin-7-(6"'-p-coumarylsophoroside), 8-hydroxyluteolin 8-glucoside, luteolin 7-rhamnosyl(1-6)galactoside, along with 10-hydroxyyohimbine showed great potential as leads for developing new antibacterial agents.

1. Introduction

Antimicrobial resistance (AMR) is a global crisis with profound health and economic implications. In response to its escalating impact, the World Health Organization (WHO) established a global research agenda that prioritizes critical bacterial pathogens, with key updates released in 2015, 2017, and most recently in 2024 (Bertagnolio *et al.*, 2024). Apart from this, the landmark 2014 Review on Antimicrobial Resistance projected that AMR could lead to as many as 10 million deaths every year by 2050, if not mitigated (O'Neill, 2016). These alarming forecasts underscore the critical urgency for sustained research and innovation in the development and advancement of novel antimicrobial agents.

***Corresponding author**
E-mail address: quahmed@iium.edu.my (QU Ahmed)

Received: 14 July, 2025 **Accepted:** 04 October, 2025 **Published:** 06 December, 2025

DOI: 10.25259/JKSUS_1185_2025

Microbial infections, particularly those related to the mouth, are produced by pathogenic microbes such as viruses, bacteria, and fungi that inhabit the oral cavity and often form biofilms (Flemming *et al.*, 2016). These biofilms can trigger inflammatory responses and contribute to disease progression in dysbiosis-related conditions (Goodman *et al.*, 2018). If left untreated, chronic oral infections may escalate to oral cancer owing to the roles of pathogenic microbes like *Streptococcus mutans* and *Staphylococcus aureus* in carcinogenesis (Odunitan *et al.*, 2024; Yu *et al.*, 2022). Although *Escherichia coli* is typically localized in the gastrointestinal tract, it can become life-threatening in immunocompromised individuals (Tao *et al.*, 2020). Thus, it's very crucial to treat these infections timely and effectively to avoid the progression to oral cancer, despite the growing resistance of oral biofilms to conventional antibiotic therapies (Kenganora *et al.*, 2021). Additionally, the existing synthetic drugs offer toxicity, side effects, and drug resistance (Umar *et al.*, 2022). These limitations highlight the urgent need for alternative therapeutic strategies. Traditional medicinal plants, long utilized for their healing properties, are a promising avenue for novel drug discovery and development. Their rich ethnopharmacological heritage and demonstrated bioactive properties position them as promising candidates in the ongoing battle against microbial infections and the escalating threat of antibiotic resistance.

A traditional medicinal plant, viz. *Mitragyna speciosa* Korth (local name: Kratom) is native to Southeast Asia and characterized by its relatively large, oval-shaped, glossy dark green leaves (Begum *et al.*, 2025a). It has long been used by local people to manage several health conditions, including anxiety, diarrhea, pain, intestinal infections, fever, cough, diabetes, hypertension, increasing sexual stimulation, wound healing, opioid withdrawal, and cancer prevention (Begum *et al.*, 2024). Of late, the kratom leaves have spread to Western countries from their origin, where it is commercially accessible in different kinds, such as capsules, tablets, smoking preparations, and dried leaves for brewing or chewing purposes (Begum *et al.*, 2025b).

A considerable volume of scientific research has been dedicated to investigating the bioactive constituents and pharmacological effects of Kratom leaves, highlighting their potential in various therapeutic applications. These studies have been predominantly focused on alkaloids, especially with mitragynine, which is recognized as the principal bioactive compound (Bagum *et al.*, 2024). Apart from the alkaloids, a diverse array of secondary metabolites has been identified in Kratom, including triterpenoid saponins such as quinovic acid 3-O-β-D-glucopyranoside and quinovic acid 3-O-β-D-quinovopyranoside, the saponin daucosterol, and various glycoside derivatives like roseoside, vogeloside, epivogeloside, 3-oxo-α-ionyl-O-β-D-glucopyranoside, 1-O-feruloyl-β-D-glucopyranoside, and benzyl-β-D-glucopyranoside, as well as the flavonoid epicatechin. The outcomes of the pharmacological studies have revealed that Kratom leaves demonstrate a wide spectrum of biological properties, namely antioxidant activities, antimicrobial and antibiofilm effects, anticancer potential, antidiabetic activity, antiparasitic efficacy, antitussive effects, and antispasmodic actions (Begum *et al.*, 2025a).

Antioxidants such as carotenoids (xanthophylls and carotenes), anthocyanins, terpenoids, lignans, terpenoids, stilbenes, tannins, vitamins, flavonoids, and phenolic acids have the capability to counteract free radicals and reactive oxygen species (ROS) within cells (Abeyrathne *et al.*, 2022). Numerous studies have highlighted the coexistence of antioxidant and antibacterial activities in various plant-derived extracts, underscoring their therapeutic potential (Irshad *et al.*, 2025; Sitthan *et al.*, 2023). Building upon these insights, the primary objective of the present study was to investigate the antibacterial, antibiofilm, and antioxidant properties of Kratom leaf extracts, aiming to explore their efficacy as a source of bioactive compounds for potential pharmaceutical applications. Additionally, the research intended to detect the phytochemical components of the most potent bioactive extract and to perform molecular docking and ADMET (Absorption, Distribution, Metabolism, Excretion, and Toxicity) analyses to illuminate the mechanisms of action and assess the therapeutic possibility of these compounds as antibacterial agents.

2. Materials and Methods

2.1 Plant sample collection and laboratory preparation

Fresh Kratom leaves were sourced from Kedah, Malaysia, and subsequently identified and authenticated at the Kulliyyah of Pharmacy, International Islamic University Malaysia, under voucher number PIIUM 0358. The collected leaves were thoroughly washed with distilled water to remove adhering soil and debris, followed by drying at 40 °C for 3 days to preserve phytochemical integrity. The dried material was then pulverized using a Universal cutting mill (Germany) to obtain a fine powder suitable for extraction and further analysis.

2.2 Maceration-based preparation of plant extracts

The maceration was performed by immersing the powdered leaves in a series of methanol and water solvent systems (100%, 75%, 50%, 25%, and 0% methanol). Generally, 100 g of dried leaf powder was carefully shifted to a round-bottom flask, and the solvent system was added in a 1:3 powder-to-solvent ratio, and the resultant mixture was left in the dark for 24 h at room temperature. Later, filtration was performed through Whatman filter paper No. 3, and the resultant filtrate was transferred to a Buchi rotary evaporator for concentration. This process was repeated three times. Using different solvent systems, five different extracts were obtained (0% methanol M, 25% methanol M, 50% methanol M, 75% methanol M, and 100% methanol M). Here, "M" specifies an extract obtained using the maceration technique. Finally, the percentage yields of the concentrated extracts were calculated (Ananda *et al.*, 2025).

2.3 Ultrasound-assisted preparation of plant extracts

Ultrasound assisted extraction was performed by using 5 g of dried powder of Kratom leaf and 50 mL of various methanol-water solvent systems, similar to those used in maceration extraction. The mixture was placed in an ultrasound machine (JEIOTECH, UC-10) and subjected to an ultrasound-assisted extraction (UAE) for 30 min at ambient temperature. After extraction, the mixture was filtered and concentrated through a rotary evaporator. This process was repeated three times (Zhang *et al.*, 2018). Consequently, five different ultrasound extracts were obtained: 0% methanol U, 25% methanol U, 50% methanol U, 75% methanol U, and 100% methanol U. Here, "U" specifies the extracts obtained by the UAE technique. The percentage yields of the concentrated extracts were then calculated according to Ananda *et al.* (2025) by the formula shown below:

$$\% \text{ yield} = (\text{mass of dry extract})/(\text{mass of dry plant}) \times 100$$

2.4 Alkaloid and ethyl acetate fractionation

From the 100% methanol macerated extract (100% Methanol M), further fractionation was carried out to obtain the alkaloid fraction and the ethyl acetate fraction separately (Ananda *et al.*, 2025). The overall extraction and fractionation workflow for all samples derived from *M. speciosa* leaf has been illustrated in Fig. 1.

2.5 Qualitative phytochemical screening

After extraction, the 12 Kratom leaf extracts were subjected to qualitative phytochemical screenings to identify the presence of key bioactive constituents. Standard protocols were employed to detect alkaloids (Settaluri *et al.*, 2024), glycosides (Raduan *et al.*, 2022), saponins (Ananda *et al.*, 2025), terpenoids (Settaluri *et al.*, 2024), phytosterols (Noormazlinah *et al.*, 2019), as well as phenolic and flavonoid compounds (Ananda *et al.*, 2025). These assessments provided a foundational understanding of the phytochemical composition of the extracts, supporting their potential therapeutic applications.

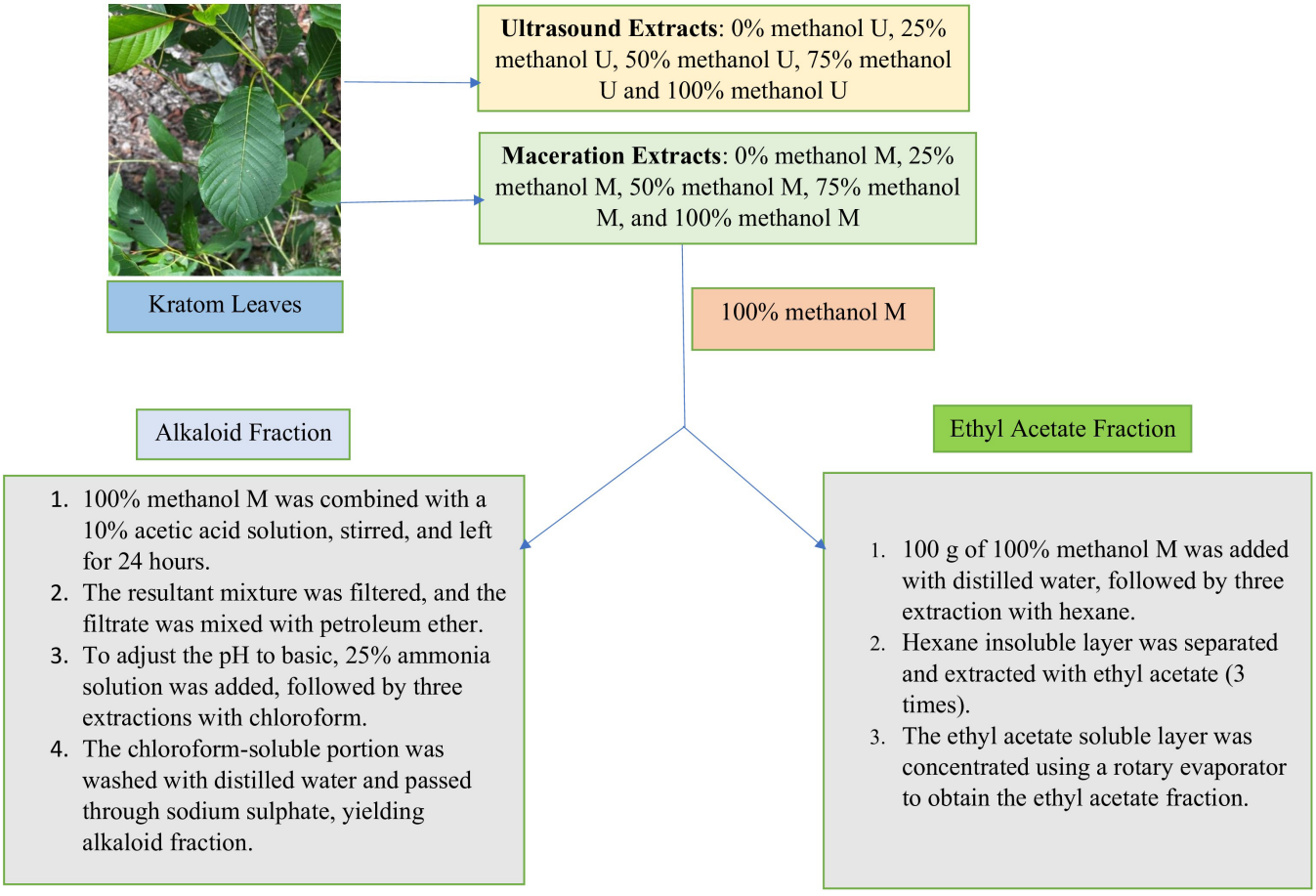

Fig. 1. Schematic overview of the extraction and fractionation workflow applied to all samples derived from *Mitragyna speciosa* leaves.

2.6 Quantitative phytochemical screening

2.6.1 Total phenolic content assay

This assay was conducted following the protocol described by Raduan *et al.* (2022), with minor modifications, utilizing the Folin-Ciocalteu (FC) method to assess total phenolic content (TPC). Gallic acid monohydrate was used at 400, 200, 100, 50, 25, 12.5, 6.25, and 3.125 µg/mL to obtain a standard calibration curve. Each extract solution had a concentration of 1 mg/mL. The solvent used to prepare the extract solution served as a control. In each well of the microplate, 20 µL of extract or 20 µL of gallic acid, or 20 µL of solvent was added to 100 µL of 10% FC reagent and well shaken, followed by incubation for 4 min at room temperature. Subsequently, 80 µL of 7.5% sodium carbonate solution was added to each well, followed by gentle agitation and incubation at room temperature for 2 h to facilitate the reaction. The absorbance of the resulting mixture was then measured at 765 nm using a microplate reader. The TPC was expressed as milligrams of gallic acid monohydrate equivalent per gram of extract (mg GAE/g), based on a standard calibration curve.

2.6.2 Total flavonoid content assay

This assay was performed following the methodology outlined by Raduan *et al.* (2022), with minor modifications. Quercetin dihydrate (98%) was used as the reference standard, prepared in serial dilutions of 200, 100, 50, 25, 12.5, 6.25, 3.125, and 1.5625 µg/mL to generate a standard calibration curve. Each extract was reconstituted at a concentration of 1 mg/mL. In a 96-well microplate, 50 µL of either the extract or standard solution was mixed with 100 µL of methanol, while the blank well contained 150 µL of methanol alone. Subsequently, 20 µL of 10% aluminum chloride ($AlCl_3$) was added to each well, followed by gentle agitation and incubation at room temperature for 3 min. This was followed by the addition of 20 µL of 1 M sodium acetate (CH_3COONa) and 60 µL of methanol. The microplates were then incubated at room temperature for 40 min, and the absorbance was measured at 415 nm using a microplate reader. The total flavonoid content (TFC) was expressed as milligrams of quercetin dihydrate equivalent per gram of extract (mg QE/g).

2.7 Antioxidant assays

2.7.1 DPPH scavenging assay

This assay was conducted in accordance with the protocol described by Raduan *et al.* (2022), with minor modifications. Ascorbic acid was employed as the reference standard, and various concentrations of both the standard and extract solutions were prepared via serial dilution from a 1 mg/mL stock solution using methanol. In a 96-well microplate, 100 µL of each diluted extract or standard solution was combined with 100 µL of 0.2 mM DPPH solution, followed by gentle shaking and incubation at room temperature for 30 min in the dark to prevent photodegradation. After incubation, the absorbance was measured at 517 nm using a microplate reader. For blank wells, 100 µL of extract or ascorbic acid was mixed with 100 µL of methanol, excluding DPPH. The control wells contained 100 µL of methanol and 100 µL of DPPH solution, while the blank control consisted of 200 µL of methanol alone. This setup enabled accurate assessment of the antioxidant activity of the extracts based on their DPPH radical scavenging capacity. The equation used to measure the DPPH scavenging activity (%) is given below:

$$(\%)\ \text{Inhibition} = (A_{control} - A_{sample})/(A_{control}) \times 100\%$$

Here, $A_{control}$= Absorbance of control; A_{sample}=Absorbance of sample (extract/standard)

2.7.2 FRAP test

This test was performed by following the procedure outlined by Raduan *et al.* (2022) with few required amendments. The solution of each extract was made in DMSO at 250 µg/mL. Various concentrations of ascorbic acid (200, 100, 50, 25, 12.5, 6.25, 3.125, and 1.5625 µg/mL) were prepared to generate a standard curve. In each well of a 96-well microplate, 30 µL of either the extract or ascorbic acid (standard) or DMSO (control) was mixed with 270 µL of freshly prepared ferric reducing antioxidant power (FRAP) reagent. The mixture was then incubated for thirty minutes at 37 °C in a dark condition to prevent light-induced degradation. Following incubation, the absorbance was measured at 593 nm using a microplate reader, enabling the evaluation of the ferric reducing antioxidant power of the samples. The FRAP activity was recorded as milligrams of ascorbic acid equivalent per gram of each sample (mg AAE/g).

2.8 Antimicrobial activity evaluation of kratom leaf extracts

Antimicrobial assessments were carried out using disc diffusion assay, broth microdilution assay, and antibiofilm test on three different pathogens, namely *Escherichia coli* (ATCC 25922), *Streptococcus mutans* (ATCC 25175), and *Staphylococcus aureus* (ATCC 25923). These bacterial strains were obtained from the Kulliyyah of Dentistry, IIUM. The bacteria were subcultured on Brain Heart Infusion (BHI) agar. Four to five colonies were picked using a sterilized wire loop from the pure cultures of *E. coli*, *S. mutans,* and *S. aureus,* and finally transferred to BHI broth. The optical densities were adjusted to OD 600 nm of 0.5 for *E. coli*, OD 620 nm of 0.5 for *S. mutans*, and OD 595 nm of 0.5 for *S. aureus* to achieve a concentration of 10^8 CFU/mL (Qiao *et al.*, 2021; Arzmi *et al.*, 2015).

2.8.1 Disc diffusion test

This assay was followed based on the method mentioned by Hossain *et al.* (2024) with a few changes. Initially, each extract was prepared in methanol at three different concentrations (100, 50, and 25 mg/mL). A 0.12% chlorhexidine solution served as the standard, while methanol was used as the negative control. Each disc was impregnated with 20 µL of extract, 0.12% chlorhexidine, or methanol, and then dried to ensure no methanol remained. The inoculation procedure was carried out by uniformly streaking standardized bacterial inocula onto the surface of Mueller-Hinton agar (MHA) plates using sterile cotton swabs to ensure even distribution. Sterile discs impregnated with the test extracts were then carefully placed onto the agar surface. The plates were subsequently incubated at 37 °C for 24 h under aerobic conditions. Following the incubation period, the zones of inhibition, indicative of antibacterial activity, were measured in millimeters using a digital caliper or ruler and recorded for further analysis. The disc diffusion test was carried out thrice.

2.8.2 MIC and MBC determination

Following the disc diffusion test, extracts that exhibited antibacterial activity were further evaluated using the broth microdilution method to ascertain the Minimum Inhibitory Concentration (MIC) and Minimum Bactericidal Concentration (MBC), based on the procedure described by Hossain *et al.* (2024) with necessary modifications. Initially, stock solutions of the extracts were prepared at a concentration of 100 mg/mL by dissolving 100 mg of the extracts in 1 mL of a methanol-phosphate buffered saline (PBS) (10:90) solvent system to enhance solubility. Serial dilutions were then performed using the same solvent system to yield eight dissimilar concentrations. In a sterile 96-well microplate, 10 µL (for *Staphylococcus aureus*) or 20 µL (for *Streptococcus mutans*) of each diluted extract was added to 90 µL (for *S. aureus*) or 80 µL (for *S. mutans*) of PBS. This was followed by the addition of 50 µL of bacterial inoculum (*S. aureus* or *S. mutans*, 10^8 CFU/mL) and 50 µL of BHI broth. The plates were incubated at 37 °C for 24 h, ensuring that the final methanol concentration did not exceed 1% to avoid solvent-induced effects. Control groups included: Extract + PBS + BHI (no bacteria), PBS + Culture + BHI (no extract), PBS + BHI (no extract or bacteria), 0.12% Chlorhexidine + PBS + Culture + BHI (positive control), and 0.12% Chlorhexidine + PBS + BHI (no bacteria). Post-incubation, MIC values were determined by adding 20 µL of 5 mg/mL MTT reagent (3-(4,5-dimethylthiazol-2-yl)-2,5-diphenyltetrazolium bromide) to each well, followed by incubation at 30 °C for 30 min. The presence of blue-coloured formazan indicated bacterial viability, and the lowest concentration that showed no color change was recorded as the MIC. To determine the MBC, a loopful of broth from wells corresponding to MIC and higher concentrations was streaked onto MHA plates, followed by incubation at 37 °C for 24 h. The lowest concentration that revealed no visible bacterial growth was recorded as the MBC.

2.8.3 Antibiofilm test

2.8.3.1 Static biofilm formation

The antibiofilm activities of *M. speciosa* leaf extracts against *S. mutans* and *S. aureus* biofilms were investigated based on the procedure outlined by Famuyide *et al.* (2019) with necessary adjustments. The extract solutions were formulated using the identical solvent system utilized in the broth microdilution procedure. For each extract, two concentrations were tested: 1xMIC and 2xMIC. In a sterile 96-well microplate, the appropriate volume of extract solution was combined with PBS, 50 µL of bacterial suspension (10^8 CFU/mL), and 50 µL of BHI broth, resulting in a final volume of 200 µL per well. The experimental setup included the following controls: Extract + PBS + BHI (no bacteria), PBS + Culture + BHI (no extract), PBS + BHI (no extract or bacteria), 0.12% Chlorhexidine + PBS + Culture + BHI (positive control), and 0.12% Chlorhexidine + PBS + BHI (no bacteria). The plates were incubated at 37 °C for 72 h, with the culture medium replaced aseptically every 24 h to maintain optimal growth conditions and prevent nutrient depletion.

2.8.3.2 Crystal violet test

Upon the incubation period, the plates were carefully washed with sterilized distilled water to eradicate the planktonic cells. The plates were then dried in a biosafety cabinet. Once dried, 200 µL of 100% methanol was added to each well and left for 20 min. The methanol was then removed, and 200 µL of 0.1% crystal violet solution was added and retained for 20 min. Excess stain was washed off with distilled water, and 200 µL of 100% ethanol was added to destain the wells. After 20 min, 100 µL of destaining solution was collected from each well and transferred to a new microplate. The absorbance of each well was measured at 590 nm using a microplate reader. The mean absorbance values of the samples were calculated, and the biofilm inhibition was expressed as percentage inhibition using the following equation:

(%) Inhibition = (OD (Negative control)- OD(Sample))/(OD (Negative control)) ×100%

2.9 Q-TOF-LCMS analysis for bioactive compounds identification of M. speciosa leaf extract

The most potent extract exhibiting antibacterial activity was further evaluated through a liquid chromatography-mass spectrometry-quadrupole time-of-flight (LCMS-QTOF) instrument (Agilent 1290 Infinity and 6550 iFunnel, Santa Clara, CA, USA). The sample was prepared by dissolving 1 mg of Kratom extract in 250 µL of LC-grade MeOH, followed by vortexing, sonication, and subsequent mixing with 250 µL of distilled H_2O. The resulting solution was centrifuged for almost 15 min, and the supernatant was collected and filtered into a vial made of glass for analysis. Chromatographic separation was performed using a C18 column (Phenomenex Kinetex) kept at 27°C, with a gradient elution preparatory from 5% MeOH in H_2O containing 0.1% methanoic acid to absolute MeOH over 20 min, followed by 10 min of isocratic elution with absolute methanol at a flow rate of 0.0007 L/min. The MS data were attained in the m/z range of 50-1500, employing a collision energy ramp of 35 eV. The data developed were managed through different specific software including ACD/Spec Manager and MZmine (Ananda *et al.*, 2025).

2.10 Molecular docking

The detected compounds of the ethyl acetate fraction were checked through the molecular docking method. The structures of chlorhexidine (standard) and the detected compounds were retrieved from https://pubchem.ncbi.nlm.nih.gov/. The target protein corresponding to the GyrB ATPase domain of *S. aureus* (PDB ID: 3U2D) was retrieved from accessing the http://www.rcsb.org (Protein Data Bank). By adjusting the grid coordinates, i.e., X: 0.548, Y: 2.587, and Z: 23.537, the native ligand was redocked to ensure an RMSD (root-mean-square deviation) below two Å. AutoDock Vina, Autodock Tools 1.5.7, and Discovery Studio software. Docking results were analyzed through both 2D and 3D visualizations to better understand observations of the binding sites interactions (Hossain *et al.*, 2024; Eakin *et al.*, 2012; Ananda *et al.*, 2025).

2.11 Physico-chemical and pharmacokinetic properties

Studying physicochemical and pharmacokinetic properties is indispensable for envisaging the behavior of a drug in the human body, adjusting its beneficial effects, and ensuring its safety. Hence, bioactive compounds of the ethyl acetate fraction were further checked for their effect on drug absorption and distribution. These properties also affect how a drug is metabolized by the liver and other organs, as well as how quickly it is cleared from the body (Ananda *et al.*, 2025) (www.swissadme.ch/index.php; biosig.lab.uq.edu.au/pkcsm/prediction).

2.12 Statistical analysis

Data generated after successfully performing all assays were statistically investigated through Minitab software version 21.4. A one-way analysis of variance (ANOVA) was done to evaluate significant differences among the groups. Tukey's post hoc multiple comparison test was applied to identify specific pairwise differences between group means at a significance level of $p < 0.05$.

3. Results & Discussion

3.1 Percentage of extract yield and qualitative phytochemical screening of kratom leaf extracts

Extraction marks the preliminary phase in isolating bioactive compounds from natural sources such as leaves, stems, flowers, or roots. Among the various existing extraction techniques, maceration remains a traditional extraction method, particularly well-suited for thermolabile compounds. This process involves soaking plant material at room temperature for an extended duration, enabling the gradual diffusion of phytoconstituents from the solid matrix into the solvent. Despite its simplicity, maceration is time-consuming and demands a substantial volume of solvent. In contrast, UAE offers a faster and more efficient extraction alternative, enhancing mass transfer through acoustic cavitation, thereby reducing extraction time and solvent usage. It employs ultrasonic waves to facilitate the dissolution and diffusion of compounds in a comparatively smaller amount of solvent. Thus, UAE can bring the compounds that may not dissolve in the normal maceration method due to limited solubility. Several factors influence extraction efficiency, including temperature, type of solvent, the ratio of plant material (leaf, stem, flower, or root) to solvent, and extraction time. These factors can significantly affect the extraction efficiency, yield, composition, as well as the type of compounds extracted (Li *et al.*, 2014; Zhang *et al.*, 2018; Al Ubeed *et al.*, 2022).

In this research, initially, both maceration and UAE methods were used to generate two sets of extracts, each using five different methanol-water solvent systems. Methanol, a multipurpose solvent, is proficient in removing both polar and nonpolar constituents from plants. Previous studies have also observed that methanol extract often exhibits more potent antioxidant activity compared to other solvents, with more methanol ratios correlating with increased total phenolic compound content (Moneim *et al.* 2022; Riyadi *et al.*, 2023). Thus, the use of five methanol-water ratios enabled the extraction of compounds with varying polarities, resulting in five distinct extract types to perform the subsequent qualitative phytochemical screening. As presented in the supplementary file (Table S1), the extracts obtained post-extraction exhibited variable yield percentages and distinct profiles of phytochemical components.

3.2 Quantitative phytochemical screening and antioxidant tests

The quantitative phytochemical (TPC, TFC) and antioxidant (DPPH, FRAP) tests were performed on three groups of extracts comprising 12 different extracts and fractions. Numerous studies have established the fact that the plant's constituents, namely phenolic and flavonoid compounds, are quite strong in terms of exhibiting antioxidant properties (Wang *et al.*, 2021). This correlates the highest TPC and TFC values of the extracts with their high antioxidant property, especially 100% methanol M extract, 100% methanol U extract, and ethyl acetate fraction. A range of tests with distinct mechanisms of action is available to check the antioxidant effects of the extracts or isolated compounds. In this study, two widely used methods, namely DPPH and FRAP tests, were used to check the antioxidant potential. In fact, the DPPH assay utilizes the stable free radical DPPH•, and measures antioxidant property based on the compound or extract capacity to neutralize this DPPH free radical. This method is particularly suited for detecting hydrophobic antioxidants. In contrast, the FRAP assay is a rapid, simple, and cost-effective method designed to measure the antioxidant capacity of hydrophilic compounds. It operates by quantifying the capability of an extract or a compound to reduce ferric ions (Fe^{3+}) to ferrous ions (Fe^{2+}) at low pH, reflecting their electron-donating potential as an antioxidant (Sarian *et al.*, 2017; Ahmed *et al.*, 2018). Thus, by incorporating both assays, the current study measures the antioxidant activity of both hydrophobic and hydrophilic constituents present in the extracts to get a comprehensive idea of their antioxidant potential. The results of the quantitative phytochemical analyses (TPC, TFC) and antioxidant evaluations (DPPH, FRAP), statistically assessed within each extract group, have been shown in Table 1.

Among the maceration extracts, the 100% methanol M showed the highest activity in all four tests: (TPC: 257.46 ± 1.32 mg GAE/g extract, $p < 0.05$, TFC: 50.75 ± 0.24 mg QE/g extract, $p < 0.05$, DPPH: IC50 7.94 ± 0.12 µg/mL, $p < 0.05$ and FRAP: 2103.46 ± 5.67 mg AAE/g extract, $p < 0.05$). Similarly, among the ultrasonic extracts, the 100% methanol U showed the highest activity in all four tests: (TPC: 340.99 ± 2.38 mg GAE/g extract, $p < 0.05$, TFC: 62.95 ± 0.77 mg QE/g extract, $p < 0.05$, DPPH: IC50 7.57 ± 0.24 µg/mL, $p < 0.05$ and FRAP: 2365.99 ± 3.39 mg AAE/g extract, $p < 0.05$). Conversely, between the specialized extracts obtained from 100% methanol M extract, the ethyl acetate fraction showed better activity than the alkaloid fraction: TPC (337.00 ± 19.60 mg GAE/g extract, $p < 0.05$), TFC (57.72 ± 3.79 mg QE/g extract, $p < 0.05$), DPPH (IC50 15.03 ± 0.54 µg/mL) and FRAP (2981.7 ± 40.6 mg AAE/g extract, $p < 0.05$). The alkaloid-rich fraction was specifically prepared to ensure a higher concentration of alkaloids relative to other phytochemical constituents, such as phenolics and flavonoids. Thus, this fraction showed lower TPC and TFC, which corresponded with a reduced antioxidant capacity. These findings clearly underscore the significant contribution of phenolic and flavonoid compounds to the overall antioxidant property of the extracts.

According to Jadid *et al.* (2017), antioxidant activity in the DPPH assay is classified as strong when IC_{50} values fall between 10 and 50 µg/mL, moderate when ranging from 50 to 100 µg/mL, and weak when exceeding 100 µg/mL. In our study, both the 100% methanol M and 100% methanol U extracts demonstrated IC_{50} values within the strong activity range and comparable to that of the ascorbic acid (standard antioxidant). This correlates with the highest TPC and TFC values of the 100% methanol M extract, 100% methanol U extract, and ethyl acetate fraction, with the highest antioxidant property observed.

3.3 Antibacterial assay

The disc diffusion test was performed with twelve different extracts of *M. speciosa* leaf at three different concentrations each, against *E. coli*, *S. mutans* and *S. aureus* which offered low cost, flexibility, and short processing time (Coorevits *et al.*, 2015) and helped in selecting the extracts for subsequent tests. The outcomes of disc diffusion test

Table 1.
Results of quantitative phytochemical tests and antioxidant tests for *M. speciosa* leaf extracts and fractions.

Extract/ Fraction/ Standard	Quantitative assay		Antioxidant assay	
	TFC (mg QE/g of extract)	TPC (mg GAE/g of extract)	DPPH (IC_{50} µg/mL)	FRAP (mg AAE/g of extract)
Maceration extracts				
0% methanol M	28.59 ± 0.61^{e}	139.51 ± 0.75^{e}	22.48 ± 0.57^{a}	1249.54 ± 8.86^{e}
25% methanol M	31.50 ± 0.17^{d}	160.44 ± 1.15^{d}	20.84 ± 0.36^{b}	1567.33 ± 6.66^{d}
50% methanol M	39.70 ± 1.38^{c}	189.70 ± 1.32^{c}	12.51 ± 0.10^{c}	1851.58 ± 1.39^{c}
75% methanol M	43.94 ± 1.29^{b}	205.00 ± 1.16^{b}	8.86 ± 0.09^{d}	1942.17 ± 10.65^{b}
100% methanol M	50.75 ± 0.24^{a}	257.46 ± 1.32^{a}	7.94 ± 0.12^{e}	2103.46 ± 5.67^{a}
Ascorbic acid	NA	NA	5.26 ± 0.03^{f}	NA
Ultrasonic extracts				
0% methanol U	18.10 ± 0.36^{e}	256.32 ± 0.78^{e}	26.06 ± 0.20^{a}	1454.74 ± 1.81^{e}
25% methanol U	26.87 ± 1.71^{d}	268.51 ± 1.38^{d}	13.77 ± 0.18^{b}	2069.08 ± 2.00^{d}
50% methanol U	35.25 ± 1.40^{c}	279.46 ± 4.23^{c}	12.21 ± 0.13^{c}	1832.00 ± 21.6^{c}
75% methanol U	49.21 ± 0.31^{b}	296.59 ± 3.33^{b}	11.72 ± 0.12^{d}	2208.50 ± 37.0^{b}
100% methanol U	62.95 ± 0.77^{a}	340.99 ± 2.38^{a}	7.57 ± 0.24^{e}	2365.99 ± 3.39^{a}
Ascorbic acid	NA	NA	5.26 ± 0.03^{f}	NA
Other fractions				
Alkaloid fraction	29.47 ± 0.70^{b}	82.130 ± 0.60^{b}	106.13 ± 10.95^{a}	541.71 ± 3.30^{b}
EtOAc fraction	57.72 ± 3.79^{a}	337.00 ± 19.60^{a}	15.03 ± 0.54^{b}	2981.70 ± 40.6^{a}
Ascorbic acid	NA	NA	5.26 ± 0.03^{b}	NA

Results are presented as mean ± standard deviation (SD). Means not sharing the same letter indicate statistically significant differences ($p < 0.05$).

revealed that only 100% methanol M extract, 100% methanol U extract, and ethyl acetate fraction showed zones of inhibition at all concentrations. For *S. mutans*, only the 100% methanol M extract, 100% methanol U extract and ethyl acetate fraction showed zones of inhibition at 50 and 100 mg/mL. However, none of the extracts and fractions at any concentration exhibited ZOI against *E. coli*. The findings of the disc diffusion test results were compared with the results of 0.12% chlorhexidine within the same extract group. Against *S. aureus*, all three extracts showed significantly different zones of inhibition. However, against *S. mutans*, in all three extracts, the zone of inhibition was not significantly different at 50 and 100 mg/mL.

Based on the outcomes of the disc diffusion test, 100% methanol M extract, 100% methanol U extract, and ethyl acetate fraction were selected to investigate their MIC and MBC against *S. aureus* and *S. mutans* through the broth microdilution test. During the broth microdilution assay, the extracts demonstrated partial solubility in water-based solvents, leading to precipitation upon the addition of broth into the wells. Moreover, the inherent colors of the extracts interfered with visual assessment, posing a challenge in accurately determining the MIC. To address these issues, a methanol-PBS solvent system was used, along with the MTT colorimetric method to visually identify the MIC well, as suggested by Veiga *et al.* (2019). The results showed that the ethyl acetate fraction displayed a minimum bactericidal effect at 5 mg/mL against *S. aureus*. Among the tested fractions, the ethyl acetate fraction demonstrated the most potent antibacterial activity, with MIC values of 1.25 mg/mL against *S. aureus* and 2.5 mg/mL against *S. mutans*. Moreover, it was the only fraction to demonstrate an MBC at 5 mg/mL against *S. aureus*, indicating its superior bactericidal efficacy (Fig. S1). The findings of the disc diffusion and broth microdilution tests have been shown in Table 2.

The three extracts were further subjected to antibiofilm tests to evaluate their potential to inhibit biofilm formation. In this regard, two concentrations (1xMIC and 2xMIC of the respective extracts) were used. The outcomes of the antibiofilm test indicated a reduction in biofilm biomass and an increase in inhibition with higher extract concentrations. Statistical analysis was conducted to evaluate the efficacy of the extracts, wherein the biofilm biomass of each extract-treated group was compared to that of the untreated control, and the percentage inhibition was assessed relative to the standard treatment (0.12% chlorhexidine), as presented in Table 3. The differences observed were statistically significant ($p < 0.05$). Notably, the 100% methanol maceration extract, 100% methanol ultrasonication extract, and the ethyl acetate fraction demonstrated significant activity against both the planktonic and biofilm forms of *S. aureus* and *S. mutans*.

In accordance with the findings from planktonic evaluations, the Kratom leaves extracts exhibited pronounced antibiofilm effect against pathogenic *S. aureus*, while its impact on *S. mutans* was comparatively attenuated. Markedly, this is the first report highlighting the antibiofilm activity of the Kratom leaf extract against pathogenic microbe viz. *S. mutans*. Despite biofilm inhibition remaining less than 50% at the highest tested dose, this type of outcome aligns with the behavior of many phytoconstituents isolated from medicinal plants, which frequently exert their activities via intricate, multi-targeted pathways distinct from conventional antibiotic mechanisms. Unlike conventional antibiotics that exert potent bactericidal effects, plants extract often disrupt biofilm formation through alternative mechanisms, namely quorum sensing interference, glucosyltransferases (GTFs) (key enzymes in *S. mutans* biofilm development) inhibition, and destabilization of the extracellular polymeric substance (EPS) matrix pathways that may not be responsible for high percentage of inhibitions initially despite the facts that evidence supports this incongruity (Atazhanova *et al.*, 2024). A study in which it was revealed that targeting GTFs can compromise biofilm integrity even with minimal impact on planktonic growth. *In silico* findings demonstrated strong interactions of phytoconstituents against GTFs, efficiently weakening biofilm architecture and

Table 2.
Antibacterial activity of *Mitragyna speciosa* leaf extracts and fractions against *Escherichia coli*, *Streptococcus mutans*, and *Staphylococcus aureus.*

Extract/Fraction/ Control	Antibacterial Activity												
	ZOI (mm)									Broth Microdilution (mg/mL)			
	S. aureus			*S. mutans*			*E. coli*			*S. aureus*		*S. mutans*	
	25 mg/mL	50 mg/mL	100 mg/mL	25 mg/mL	50 mg/mL	100 mg/mL	25 mg/mL	50 mg/mL	100 mg/mL	MIC	MBC	MIC	MBC
100% methanol U	7.33 ± 0.29^{d}	8.50 ± 0.5^{c}	9.83 ± 0.29^{b}	-	6.67 ± 0.17^{b}	7.39 ± 0.10^{b}	-	-	-	5	-	5	-
100% methanol M	7.94 ± 0.10^{d}	8.78 ± 0.26^{c}	9.89 ± 0.10^{b}	-	6.56 ± 0.10^{b}	7.22 ± 0.19^{b}	-	-	-	5	-	10	-
EtOAc Fraction	8.11 ± 0.35^{d}	9.17 ± 0.29^{c}	12.00 ± 0.33^{b}	-	7.33 ± 0.17^{b}	8.22 ± 0.10^{b}	-	-	-	1.25	5	2.5	-
Chlorhexidine	21.89 ± 0.51^{a}			20.11 ± 0.69^{a}			20.89 ± 1.39			NA	NA	NA	NA

Note: ZOI: Zone of Inhibition.; (-): Absence. Results are presented as mean ± standard deviation (SD). Means not sharing the same letter indicate statistically significant differences ($p < 0.05$).

Table 3.
Effects of kratom extracts and 0.12% chlorhexidine on biofilm biomass of *Staphylococcus aureus* and *Streptococcus mutans*.

Extracts/ fractions	Biofilm biomass											
	S. aureus						*S. mutans*					
	Concentrations (mg/mL)	Biomass (extract)	Biomass (Neg. Control)	Biomass (0.12% chlorhexidine)	% inhibition of extracts	% inhibition of 0.12% chlorhexidine	Concentrations (mg/mL)	Biomass (extract)	Biomass (Neg. Control)	Biomass (0.12% chlorhexidine)	% inhibition of extracts	% inhibition of 0.12% chlorhexidine
100% methanol M	5	0.059 ± 0.002[b]	0.523 ± 0.002[a]	NG	88.68 ± 0.40[c]	100 ± 0.0[a]	10	0.092 ± 0.002[b]	0.186 ± 0.006[a]	NG	22.97 ± 1.28[c]	100 ± 0.0[a]
	10	0.032 ± 0.002[c]			93.96 ± 0.33[b]		20	0.071 ± 0.003[c]			40.62 ± 2.11[b]	
100% methanol U	5	0.059 ± 0.002[b]			88.74 ± 0.38[c]		5	0.087 ± 0.003[b]			26.89 ± 2.52[c]	
	10	0.017 ± 0.004[c]			96.65 ± 0.83[b]		10	0.074 ± 0.001[c]			38.095 ± 0.49[b]	
EtOAc Fraction	1.25	0.062 ± 0.005[b]			88.04 ± 0.89[c]		2.5	0.088 ± 0.003[b]			26.05 ± 2.52[c]	
	2.5	0.032 ± 0.002[c]			93.78 ± 0.40[b]		5	0.077 ± 0.002[c]			35.57 ± 1.75[b]	

Note: NG means No Growth. Results are presented as Mean ± SD. Means having distinct letters are considered as significantly different.

pathogenicity despite lower MIC values. Hence, the antibiofilm property of *M. speciosa* leaf extract remains pertinent, mainly for biofilm-related mouth infections where conventional antibiotics frequently become ineffective owing to poor biofilm penetration and resistance (Bartels *et al.*, 2025).

3.4 Q-ToF-LCMS analysis

This analysis provided a solid baseline for identifying putative compounds in the ethyl acetate fraction. Kratom is a complex mixture of phytochemical components, including alkaloids, phenolics, flavonoids, saponins, and glycosides (Begum *et al.*, 2025a). Consequently, the above analysis of the ethyl acetate fraction identified various phytoconstituents, including alkaloids, saponins, glycosides, phenolics, and flavonoids. Some of these phytoconstituents have already been confirmed for their antioxidant and antibacterial properties. The positive and negative ionization modes chromatograms of the ethyl acetate fraction have been included in Fig. S2. The identified compounds in the *M. speciosa* leaf ethyl acetate fraction have been summarized in Table S2. Moreover, the structures of some of the key detected phytoconstituents have been illustrated in Fig. 2.

Kaempferol 3-(6"-p-coumarylglucoside)-7-glucoside, robinetin 3-rutinoside, ent-Fisetinidol-4beta-ol, 6-hydroxyluteolin 5-rhamnoside, 8-hydroxyluteolin 8-glucoside, 6-hydroxyluteoin-7-(6'''-p-coumarylsophoroside), luteolin 7-rhamnosyl(1->6) galactoside, epifisetinidol-4alpha-ol, and scutellarein 7-glucoside were some of the phenolics and flavonoids identified. Luteolin (5,7,3′,4′-tetrahydroxyflavone), a flavone subclass of flavonoids, possesses antibacterial and antibiofilm activity against *S. aureus* (MIC: 16-32 µg/mL) and *Listeria monocytogenes* (MIC: 32-64 µg/mL) (Qian *et al.*, 2020). Moreover, the antioxidant and antibacterial activities of rutin have been documented by Almuhanna *et al.* (2024) and Wang *et al.* (2021). Furthermore, the antimicrobial activity of "fisetin" against *Listeria monocytogenes* and *Streptococcus suis* has been reported by Antika and Dewi (2021), suggesting that epifisetinidol-4alpha-ol and ent-Fisetinidol-4beta-ol might possess antibacterial activity due to the presence of the "fisetin" moiety.

Reserpic acid, is believed to undergo biotransformation into reserpine within the body. Notably, reserpine has been shown to retard biofilm formation and decrease the virulence of *S. aureus* (Parai *et al.*, 2020). In parallel, the alkaloid mitragynine has demonstrated promising antioxidant and antiparasitic effects (Begum *et al.*, 2025b). In this context, Q-ToF LC-MS analysis of the ethyl acetate fraction derived from the 100% methanolic extract (Maceration extract) revealed the presence of pharmacologically active phytoconstituents that may be responsible for the observed antibacterial effects.

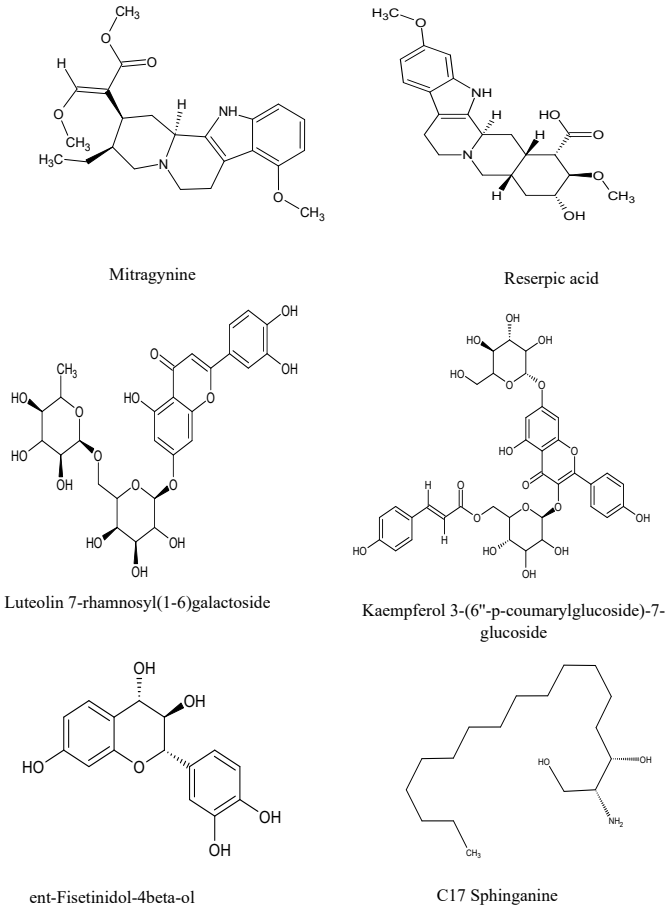

Fig. 2. Chemical structures of some compounds covering diverse chemical classes identified via Q-ToF-LCMS analysis in the ethyl acetate fraction of *Mitragyna speciosa* leaves, obtained from a 100% methanol macerated extract.

3.5 Molecular docking analysis

Q-ToF-LCMS analysis was employed to identify the bioactive compounds present in the ethyl acetate fraction of *M. speciosa* leaves. A total of 14 compounds were detected and subsequently subjected to a molecular docking study through an *in silico* approach to assess their binding affinities against the GyrB ATPase domain of *S. aureus*

(PDB ID: 3U2D). As a validation step, control docking of the native ligand (08B1) yielded a root-mean-square deviation (RMSD) of 0.823 Å and a binding energy of -7.6 kcal/mol. Additionally, chlorhexidine, used as a reference compound, demonstrated a binding score of -8.1 kcal/mol. Notably, several phytochemicals exhibited stronger binding affinities than both the native ligand and chlorhexidine: 6-hydroxyluteoin-7-(6'''-p-coumarylsophoroside) (-9.7 kcal/mol), kaempferol 3-(6"-p-coumarylglucoside)-7-glucoside (-9.6 kcal/mol), luteolin 7-rhamnosyl(1-6)galactoside (-9.3 kcal/mol), and reserpic acid: -9.1 kcal/mol. These findings suggest that selected compounds from kratom may possess promising inhibitory potential against the GyrB ATPase domain of *S. aureus*. The comprehensive results of the *in silico* molecular docking study have been presented in Table 4. Detailed binding interactions between the 3U2D protein and selected compounds: 6-hydroxyluteoin-7-(6'''-p-coumarylsophoroside), kaempferol 3-(6"-p-coumarylglucoside)-7-glucoside, luteolin 7-rhamnosyl(1-6) galactoside, reserpic acid, as well as the native ligand (08B1) and chlorhexidine have been visually depicted in Fig. 3. Additional docking interactions involving the remaining compounds have been provided in Fig. S3 within the supplementary materials.

According to Eakin *et al.* (2012), the catalytic site of the target protein (PDB ID: 3U2D) comprises key amino acid residues, including ASP81, ARG84, ARG144, and THR173. The compounds identified in this study (Table S2) showed different types of molecular interactions (bond types), such as hydrogen bonding, hydrophobic contacts, and electrostatic interactions with these catalytic residues, as well as with additional amino acids within the active site region. In the native ligand-protein interaction, ASP81 played a key role by forming a conventional hydrogen bond. Additionally, six other amino acid residues (VAL79, ILE175, ILE51, THR173, ASN54, and ILE86) contributed to the binding through various non-covalent interactions, such as hydrophobic contacts and van der Waals forces. In contrast, the compound 6-hydroxyluteoin-7-(6'''-p-coumarylsophoroside) established conventional hydrogen bonds primarily with SER129, ILE102, and SER128, indicating a distinct interaction profile compared to the naive ligand. Additionally, kaempferol 3-(6"-p-coumarylglucoside)-7-glucoside formed conventional hydrogen bonds with GLY85, ARG84, and ASN54, indicating strong interactions within the active site. Similarly, 8-hydroxyluteolin 8-glucoside exhibited hydrogen bonding with ASN54, GLU58, ARG84, and GLY85, suggesting a comparable binding profile. In contrast, the standard (chlorhexidine) formed hydrogen bonds with ILE102, ASN54, and ASP57, while other residues, ILE51, ILE175, ASP57, and GLU58 were involved in additional non-covalent interactions such as hydrophobic contacts and electrostatic forces. These findings highlight the diverse binding mechanisms employed by both natural compounds and standard drugs, contributing to their respective bioactivities.

It's noteworthy that, *in silico*, chlorhexidine didn't show interactions with any of the catalytic amino acids of the target protein, despite exhibiting potent antibacterial effects against the tested bacterial strains. This observation suggests that compounds lacking direct interactions with catalytic amino acid residues, yet sharing similar binding profiles with chlorhexidine, may also possess significant antibacterial potential. For instance, luteolin 7-rhamnosyl (1-6) galactoside showed high binding affinity through hydrogen bonds with ILE51, ILE175, ASP57, and GLU58, along with additional interactions involving ILE86. The *in silico* approach serves as a valuable predictive tool for assessing potential ligand-protein interactions, offering insights that complement *in vitro* and *in vivo* findings. Accordingly, the compounds were evaluated not only based on their computational binding results but also on their interaction similarity to chlorhexidine, reinforcing their potential as effective antibacterial agents. DNA gyrase is an essential bacterial enzyme belonging to the topoisomerase family, which plays a central role in DNA replication, transcription, and repair by modulating the supercoiling and topology of DNA (Belounis *et al.*, 2025). Due to its essential function in maintaining DNA integrity and

Table 4.
Molecular docking profile of compounds identified in the ethyl acetate fraction of Kratom leaves against the 3U2D Protein.

#	Phytoconstituents	Ligand-receptor interaction score (Predicted binding energy; kcal/mol)	Interactions with bond distance (Å)	
			Hydrogen binding interaction	Other binding interactions
1.	ent-Fisetinidol-4beta-ol	-8.2	GLY85: 2.06; THR173: 2.39; ASP81: 3.08; ASN54: 3.04	ILE86: 3.94 & 5.01
2.	Epifisetinidol-4alpha-ol	-8.1	GLU58: 3.09	ILE175: 5.13; ILE51: 5.09; ILE86: 4.00 & 4.98
3.	10-hydroxyyohimbine	-8.2	GLU58: 2.99; ARG84: 3.02; ASN54: 2.34	ILE175: 4.73; LEU103: 5.18; ILE51: 4.59; ILE86: 4.43 & 5.43; GLU58: 4.00
4.	Robinetin 3-rutinoside	-8.8	ASN54: 2.05, 2.38, 2.75, 2.39, 2.62 & 2.02; ARG144: 2.38; SER55: 2.65	ILE86: 4.93 & 5.02; ASN54: 3.94; GLU58: 4.95; ARG84: 4.35; PRO87: 5.25 & 4.13
5.	8-hydroxyluteolin 8-glucoside	-8.8	ASN54: 3.32; GLU58: 3.05; ARG84: 2.78; GLY85: 2.52	GLU58: 4.26; PRO87: 5.44; ILE86: 4.66 & 3.60
6.	Luteolin 7-rhamnosyl (1-6) galactoside	-9.3	ASN54: 3.23; VAL130: 2.83; SER129: 3.12 & 3.01	ILE86: 3.48
7.	Scutellarein 7-glucoside	-8.4	GLU58: 2.85; ASN54: 2.02; SER128: 2.76; ILE102: 2.18	ILE86: 3.46, 4.87 & 3.99
8.	Reserpic acid	-9.1	GLU58: 2.64	ILE86: 3.42 & 3.97; ILE51: 5.39
9.	6-Hydroxyluteolin 5-rhamnoside	-8.4	SER129: 1.99; ARG84: 2.31 & 2.47	GLY85: 4.76; ILE86: 3.50 & 4.25; ILE102: 5.41; ILE51: 5.28; LEU103: 5.10
10.	6-Hydroxyluteoin-7-(6'''-p-coumarylsophoroside)	-9.7	SER129: 2.25; ILE102: 3.22; SER128: 2.38; GLY 85: 2.31 & 3.00; THR173: 2.13	ASP57: 4.90 & 4.27; GLU58: 3.91; ILE86: 5.13; ILE102: 3.47
11.	Kaempferol 3-(6"-p-coumarylglucoside)-7-glucoside	-9.6	GLY85: 2.23; ARG84: 2.95; ASN54: 2.20 & 2.77; ARG144: 2.47	ASN54: 5.01; ILE86: 3.92; ALA98: 4.71; PRO87: 5.06; ILE102: 4.99 & 4.70
12.	Mitragynine	-7.0	-	VAL79: 4.61; ILE175: 4.32 & 5.15; ILE51: 4.98 & 5.18; ILE86: 3.65 & 3.86; ASN54: 5.12
13.	Phytosphingosine	-5.6	ILE102: 3.34; ASN54: 3.25 & 3.23	ILE102: 4.89; ILE86: 4.12 & 5.05; ILE175: 4.58; ILE51: 4.78
14.	C17 Sphinganine	-5.7	ILE51: 2.20	ILE102: 5.13; ILE86: 4.25 & 4.77; ARG84: 5.02 & 5.46; PRO87: 4.56
Controls	Native ligand (08B1)	-7.6	ASP81: 1.79	VAL79: 4.79; ILE175: 4.50 & 4.31; ILE51: 4.90 & 4.29; THR173: 3.86; ASN54: 4.71; ILE86: 5,17 & 5.47
	Chlorhexidine	-8.1	ILE102: 2.67; ASN54: 2.23, 2.70 & 2.62; ASP 57: 2.67	ILE51: 5.22; ILE175: 5.22 & 3.90; ASP57: 5.26; GLU58: 3.92

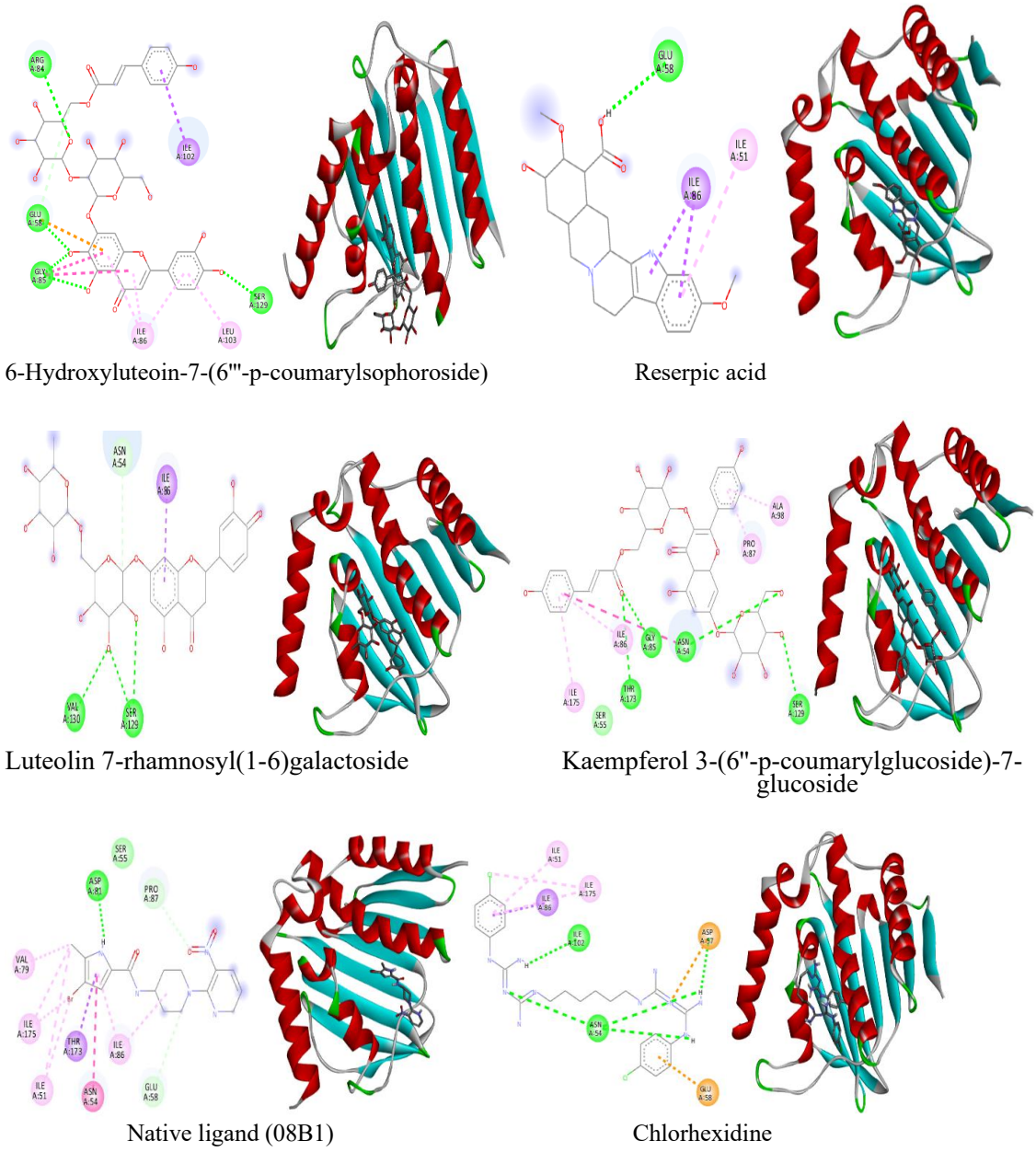

Fig. 3. The binding interactions of the native ligand, chlorhexidine, 6-hydroxyluteoin-7-(6'''-p-coumarylsophoroside), kaempferol 3-(6''-p-coumarylglucoside)-7-glucoside, luteolin 7-rhamnosyl(1-6)galactoside, and reserpic acid with the 3U2D protein.

facilitating cellular processes, inhibition of DNA gyrase disrupts these mechanisms, ultimately leading to bacterial cell death. This makes DNA gyrase a prominent target for antibacterial drug development.

3.6. Physico-chemical and pharmacokinetic properties

Based on the molecular docking results, compounds showing binding affinities equal to or higher than that of the standard (chlorhexidine: -8.1 kcal/mol) were shortlisted for further evaluation of their physicochemical and pharmacokinetic properties to assess their potential as lead candidates. Among the 11 compounds analyzed, only four compounds exhibited favorable drug likeness profiles. Of these, 10-hydroxyyohimbine showed intestinal absorption of 94.725% associated with no toxicity concerns. The remaining three compounds, namely ent-Fisetinidol-4beta-ol, Epifisetinidol-4alpha-ol, and reserpic acid, showed moderate intestinal absorption but were flagged for either AMES toxicity or hepatic toxicity (Table 5). These findings highlight the importance of integrating *in silico* pharmacokinetic screening with docking results to identify promising antibacterial leads while accounting for safety profiles.

Among the compounds evaluated, 6-hydroxyluteolin 5-rhamnoside, 6-hydroxyluteoin-7-(6'''-p-coumarylsophoroside), luteolin 7-rhamnosyl(1-6)galactoside, 8-hydroxyluteolin 8-glucoside, and kaempferol 3-(6''-p-coumarylglucoside)-7-glucoside exhibited notable molecular docking performance, demonstrating strong binding affinities and favorable interaction profiles with the target protein. However, their high polarity compromised drug-likeness by limiting intestinal absorption and bioavailability. To address this limitation, structural modification through the incorporation of hydrophobic moieties was proposed to enhance lipophilicity and improve pharmacokinetic properties. For instance, 8-hydroxyluteolin 8-glucoside and luteolin 7-rhamnosyl(1-6)galactoside can be hydrolyzed to yield the similar types of aglycones. In this aglycone structure, substitution of the four hydroxyl groups with four methoxy groups produces 5,7,3′,4′-tetramethoxyflavone, a more lipophilic derivative. This compound was subsequently evaluated using *in silico* docking, physicochemical profiling, pharmacokinetic and ADMET predictions

Table 5.
The pharmacokinetic and physicochemical characteristics of the selected phytoconstituents from *M. speciosa* leaf ethyl acetate fraction derived from the macerated 100% Methanol M leaf extract.

Phytochemical (MW)	Characteristics									
	Physicochemical Parameters					Pharmacokinetic (ADMET)				
	H-Do	H-Ac	LRV	DL	Log P	HT	IA	ROAT	AT	CLR
Kaempferol 3-(6"-p-coumarylglucoside)-7-glucoside (902.80)	12	22	3	No	-4.88	No	13.159	2.439	No	-0.293
Scutellarein 7-glucoside (448.38)	7	11	2	No	-2.10	No	45.482	2.463	Yes	0.701
Epifisetinidol-4alpha-ol (290.27)	5	6	0	Yes	-0.02	No	65.555	2.45	Yes	0.003
6-Hydroxyluteoin-7-(6'"-p-coumarylsophoroside) (772.66)	11	19	3	No	-3.64	No	17.235	2.489	No	-0.444
Reserpic acid (400.47)	3	6	0	Yes	1.08	Yes	61.972	2.1	No	0.433
6-Hydroxyluteolin 5-rhamnoside (448.38)	7	11	2	No	-1.84	No	53.78	2.556	No	0.372
ent-Fisetinidol-4beta-ol (290.27)	5	6	0	Yes	-0.02	Yes	67.556	2.115	No	0.156
Robinetin 3-rutinoside (610.52)	10	16	3	No	-3.89	No	20.596	2.49	No	-0.377
Luteolin 7-rhamnosyl(1-6)galactoside (594.52)	9	15	3	No	-3.43	No	27.777	2.734	Yes	0.251
10-hydroxyyohimbine (370.44)	3	5	0	Yes	1.66	No	94.725	2.93	No	0.885
8-Hydroxyluteolin 8-glucoside (464.38)	8	12	2	No	-2.59	No	33.475	2.562	No	0.384

Physicochemical parameters: H-Do: number of hydrogen donor; H-Ac: number of hydrogen acceptors; LRV: number of Lipinski's rule violations; DL: drug likeness; Log P: predicted octanol/water partition coefficient. Pharmacokinetic (ADMET) parameters: HT: hepatotoxicity; IA: intestinal absorption (%); AT: AMES toxicity; ROAT: rat oral acute toxicity (mol/kg); CLR: clearance; %; MW: molecular weight (gram/mole).

(Figs. S4 and S5). Although 5,7,3′,4′-tetramethoxyflavone showed somewhat lesser binding affinity (-8.3 kcal/mol) in comparison to its native counterparts, it showed excellent drug-likeness, with 98.443% of intestinal absorption and no AMES or hepatotoxicity. These findings underscore the promise of natural product derivatives as viable scaffolds for antibacterial drug development, highlighting the critical role of rational structural modification in enhancing their pharmacological properties and therapeutic efficacy (Alhassan *et al.*, 2019).

5. Conclusions

This study was initiated with the primary aim of identifying the most efficacious extract derived from *M. speciosa* leaves, based on its antioxidant and antibacterial activities. Among the twelve extracts evaluated, the ethyl acetate fraction derived from the 100% methanol M extract demonstrated superior bioactivity, highlighting the critical role of flavonoid and phenolic compounds. In contrast, the alkaloid-rich fraction, despite its high alkaloid content, showed the lowest activity, likely due to the minimal presence of phenolics and flavonoids. These findings establish a valuable foundation for future research focused on the flavonoid- and phenolic-rich fractions of kratom. Furthermore, several bioactive compounds identified within the ethyl acetate fraction, such as 6-hydroxyluteolin 5-rhamnoside, kaempferol 3-(6"-p-coumarylglucoside)-7-glucoside, 6-hydroxyluteoin-7-(6'"-p-coumarylsophoroside), luteolin 7-rhamnosyl(1-6)galactoside, and 8-hydroxyluteolin 8-glucoside, along with 10-hydroxyyohimbine exhibited promising profiles and may serve as potential lead candidates for the development of novel antioxidant and antibacterial agents with reduced toxicity. This underscores the therapeutic potential of Kratom-derived phytochemicals and supports continued exploration of its non-alkaloid constituents in drug discovery endeavors.

CRediT authorship contribution statement

Taslima Begum: Literature search, experimental studies, data acquisition, data analysis, statistical analysis, manuscript preparation; **Mohd Hafiz Arzmi:** Concepts, design, supervision, manuscript editing and review; **ABM Helal Uddin:** Supervision, manuscript editing and review; **Mohd Salleh Rofiee:** Data acquisition; **Syed Adnan Ali Shah:** Data acquisition; **Humaira Parveen:** Manuscript editing and review, data analysis; **Sayeed Mukhtar:** Manuscript editing and review, data analysis; **Qamar Uddin Ahmed:** Concepts, design, supervision, data acquisition, data analysis, statistical analysis, manuscript editing and review. All authors approved the final version of the manuscript.

Declaration of competing interest

The authors declare that they have no competing financial interests or personal relationships that could have influenced the work presented in this paper.

Declaration of Generative AI and AI-assisted technologies in the writing process

The authors confirm that there was no use of Artificial Intelligence (AI)-Assisted Technology for assisting in the writing or editing of the manuscript and no images were manipulated using AI.

Acknowledgment

The authors are grateful to Regal Malay Capital Berhad, Malaysia (SPP22-137-0137), Kulliyyah of Pharmacy, IIUM, Institute of Planetary Survival For Sustainable Well-Being (PLANETIIUM), and CPS Sejahtera Award and Research Management Centre, IIUM, Malaysia for the research support.

Appendix 1. Supplementary material

Appendix 1 (Supplementary Material): to this article can be found online at https://dx.doi.org/10.25259/JKSUS_1185_2025

References

Abdel-Moneim, A.E., El-Saadony, M.T., Shehata, A.M., Saad, A.M., Aldhumri, S.A., Ouda, S.M., Mesalam, N.M., 2022. Antioxidant and antimicrobial activities of Spirulina platensis extracts and biogenic selenium nanoparticles against selected pathogenic bacteria and fungi. Saudi J Biol Sci 29, 1197-1209. https://doi.org/10.1016/j.sjbs.2021.09.046

Abeyrathne, E.D.N.S., Nam, K., Huang, X., Ahn, D.U., 2022. Plant- and animal-based antioxidants' structure, efficacy, mechanisms, and applications: A review. Antioxidants 11, 1025. https://doi.org/10.3390/antiox11051025

Ahad Hossain, M., Sultana, S., Alanazi, M.M., Hadni, H., Bhat, A.R., Hasan, I., Kawsar, S.M.A., 2024. In vitro antimicrobial, anticancer evaluation, and in silico studies of mannopyranoside analogs against bacterial and fungal proteins: Acylation leads to improved antimicrobial activity. Saudi Pharm J 32, 102093. https://doi.org/10.1016/j.jsps.2024.102093

Ahmed, Q.U., Alhassan, A.M., Khatib, A., Shah, S.A.A., Hasan, M.M., Sarian, M.N., 2018. Antiradical and xanthine oxidase inhibitory activity evaluations of averrhoa bilimbi L leaves and tentative identification of bioactive constituents through LC-QTOF-MS/MS and molecular docking approach. Antioxidants (Basel) 7, 137. https://doi.org/10.3390/antiox7100137

Al Ubeed, H.M.S., Bhuyan, D.J., Alsherbiny, M.A., Basu, A., Vuong, Q.V., 2022. A comprehensive review on the techniques for extraction of bioactive compounds from medicinal cannabis. Molecules 27, 604. https://doi.org/10.3390/molecules27030604

Alhassan, A.M., Ahmed, Q.U., Latip, J., Shah, S.A.A., 2019. A new sulphated flavone and other phytoconstituents from the leaves of Tetracera indica Merr. and their alpha-glucosidase inhibitory activity. Nat Prod Res 33, 1-8. https://doi.org/10.1080/14786419.2018.1437427

Almuhanna, Y., Alshalani, A., AlSudais, H., Alanazi, F., Alissa, M., Asad, M., Joseph, B., 2024. Antibacterial, antibiofilm, and wound healing activities of rutin and quercetin and their interaction with gentamicin on excision wounds in diabetic mice. Biology 13, 676. https://doi.org/10.3390/biology13090676

Ananda, Z.K., Begum, T., Ahda, M., Rofiee, M.S., Shah, S.A.A., Salleh, M.Z., Almutairi, B.O., Azmi, S.N.H., Sah, P., Wardani, A.K., Khatib, A., Abbas, S.A., Mia, M.A.R., Ahmed, Q.U., 2025. Comparative evaluation of phytochemical screening, in vitro antioxidant α-Glucosidase inhibitory properties of Ceiba pentandra Basella rubra leaf extracts: Identification of active principles by Q-TOFLCMS, ADMET prediction molecular docking approach. J King Saud Univ Sci 37, 162024. https://doi.org/10.25259/JKSUS_16_2024

Antika, L.D., Dewi, R.M., 2021. Pharmacological aspects of fisetin. Asian Pac J Trop Biomed 11, 1-9. https://doi.org/10.4103/2221-1691.300726

Arzmi, M.H., Dashper, S., Catmull, D., Cirillo, N., Reynolds, E.C., McCullough, M., 2015. Coaggregation of candida albicans, actinomyces naeslundii and streptococcus mutans is candida albicans strain dependent. FEMS Yeast Res 15, fov038. https://doi.org/10.1093/femsyr/fov038

Atazhanova, G.A., Levaya, Y.K., Badekova, K.Z., Ishmuratova, M.Y., Smagulov, M.K., Ospanova, Z.O., Smagulova, E.M., 2024. Inhibition of the biofilm formation of plant streptococcus mutans. Pharmaceuticals (Basel) 17, 1613. https://doi.org/10.3390/ph17121613

Atta, L., Siddiqui, A.R., Mushtaq, M., Munsif, S., Nur-E-Alam, M., Ahmed, A., Ul-Haq, Z., 2025. Molecular insights into antibiofilm inhibitors of streptococcus mutans glucosyltransferases through in silico approaches. Sci Rep 15, 14160. https://doi.org/10.1038/s41598-025-98927-8

Bartels, N., Argyropoulou, A., Al-Ahmad, A., Hellwig, E., Skaltsounis, A.L., Wittmer, A., Vach, K., Karygianni, L., 2025. Antibiofilm potential of plant extracts: Inhibiting oral microorganisms and streptococcus mutans. Front Dent Med 6, 1535753. https://doi.org/10.3389/fdmed.2025.1535753

Begum, T., Arzmi, M.H., Khatib, A., Uddin, A.B.M.H., Aisyah Abdullah, M., Rullah, K., Mat, S.', ad, S.Z., Zulaikha Haspi, N.F., Nazira Sarian, M., Parveen, H., Mukhtar, S., Ahmed, Q.U., 2025. A review on Mitragyna speciosa (Rubiaceae) as a prominent medicinal plant based on ethnobotany, phytochemistry and pharmacological activities. Nat Prod Res 39, 1636-1652. https://doi.org/10.1080/14786419.2024.2371564

Begum, T., Arzmi, M.H., Sarian, M.N., Ali Shah, S.A., Hejaz Azmi, S.N., Uddin, A.B.M.H., Khatib, A., Ahmed, Q.U., 2025. A review on multi-therapeutic potential of the Mitragyna speciosa (kratom) alkaloids mitragynine and 7-hydroxymitragynine: Experimental evidence and future perspectives. Kuwait J Sci 52, 100381. https://doi.org/10.1016/j.kjs.2025.100381

Begum, T., Arzmi, M.H., Helal Uddin, A.B.M., Khatib, A., Abbas, S.A., Ahmed, Q.U., 2024. Mitragyna speciosa Korth toxicity: Experimental findings and future prospects. J Taibah Univ Med Sci 19, 1143-1156. https://doi.org/10.1016/j.jtumed.2024.12.002

Belounis, Y., Moualek, I., Sebbane, H., Dekir, A., Bendif, H., Garzoli, S., Houali, K., 2025. Phytochemical characterization and antibacterial activity of carthamus caeruleus l aqueous extracts: in vitro and in silico molecular docking studies. Chem Biodivers 22, e202402662. https://doi.org/10.1002/cbdv.202402662

Bertagnolio, S., Dobreva, Z., Centner, C.M., Olaru, I.D., Donà, D., Burzo, S., Huttner, B.D., Chaillon, A., Gebreselassie, N., Wi, T., Hasso-Agopsowicz, M., Allegranzi, B., Sati, H., Ivanovska, V., Kothari, K.U., Balkhy, H.H., Cassini, A., Hamers, R.L., Weezenbeek, K.V., 2024. WHO global research priorities for antimicrobial resistance in human health. Lancet Microbe 5, 100902. https://doi.org/10.1016/S2666-5247(24)00134-4

Coorevits, L., Boelens, J., Claeys, G., 2015. Direct susceptibility testing by disk diffusion on clinical samples: A rapid and accurate tool for antibiotic stewardship. Eur J Clin Microbiol Infect Dis 34, 1207-1212. https://doi.org/10.1007/s10096-015-2349-2

Eakin, A.E., Green, O., Hales, N., Walkup, G.K., Bist, S., Singh, A., Mullen, G., Bryant, J., Embrey, K., Gao, N., Breeze, A., Timms, D., Andrews, B., Uria-Nickelsen, M., Demeritt, J., Loch, J.T., Hull, K., Blodgett, A., Illingworth, R.N., Prince, B., Boriack-Sjodin, P.A., Hauck, S., MacPherson, L.J., Ni, H., Sherer, B., 2012. Pyrrolamide DNA gyrase inhibitors: Fragment-based nuclear magnetic resonance screening to identify antibacterial agents. Antimicrob Agents Chemother 56, 1240-1246. https://doi.org/10.1128/AAC.05485-11

Famuyide, I.M., Aro, A.O., Fasina, F.O., Eloff, J.N., McGaw, L.J., 2019. Antibacterial and antibiofilm activity of acetone leaf extracts of nine under-investigated south African Eugenia and Syzygium (Myrtaceae) species and their selectivity indices. BMC Complement Altern Med 19, 141. https://doi.org/10.1186/s12906-019-2547-z

Flemming, H.C., Wingender, J., Szewzyk, U., Steinberg, P., Rice, S.A., Kjelleberg, S., 2016. Biofilms: An emergent form of bacterial life. Nat Rev Microbiol 14, 563-575. https://doi.org/10.1038/nrmicro.2016.94

Goodman, B., Gardner, H., 2018. The microbiome and cancer. J Pathol 244, 667-676. https://doi.org/10.1002/path.5047

Horie, H., Chiba, A., Wada, S., 2018. Inhibitory effect of soy saponins on the activity of β-lactamases, including New Delhi metallo-β-lactamase 1. J Food Sci Technol 55, 1948-1952. https://doi.org/10.1007/s13197-018-3091-4

Irshad, A., Jawad, R., Mushtaq, Q., Spalletta, A., Martin, P., Ishtiaq, U., 2025. Determination of antibacterial and antioxidant potential of organic crude extracts from Malus domestica, Cinnamomum verum and Trachyspermum ammi. Sci Rep 15, 976. https://doi.org/10.1038/s41598-024-83506-0

Jadid, N., Hidayati, D., Hartanti, S.R., Arraniry, B.A., Rachman, R.Y., Wikanta, W., 2017. Antioxidant activities of different solvent extracts of Piper retrofractum Vahl. using DPPH assay. Proceeding of international biology conference 2016: Biodiversity and Biotechnology for Human Welfare Surabaya, Indonesia https://doi.org/10.1063/1.4985410

Kenganora, M., Rudraswamy, S., Puttabuddi Hombarvalli, J.S., Doggalli, N., 2021. Phytochemicals a novel therapeutic approach to control oral biofilm. PJ 13, 730-736. https://doi.org/10.5530/pj.2021.13.93

Li, P., Yin, Z.Q., Li, S.L., Huang, X.J., Ye, W.C., Zhang, Q.W., 2014. Simultaneous determination of eight flavonoids and pogostone in Pogostemon cablin by high performance liquid chromatography. J Liq Chromatogr Relat Technol 37, 1771-1784. https://doi.org/10.1080/10826076.2013.809545

Noormazlinah, N., Hashim, N., Nour, A.H., Abdul Munaim, M.S., Almajano, M.P., Bahirah, N., 2019. Extraction of phytosterol concentration in different legume pods by using microwave-assisted hydrodistillation. Indones J Chem 19, 796. https://doi.org/10.22146/ijc.40865

Odunitan, T.T., Apanisile, B.T., Akinboade, M.W., Abdulazeez, W.O., Oyaronbi, A.O., Ajayi, T.M., Oyekola, S.A., Ibrahim, N.O., Nafiu, T., Afolabi, H.O., Olayiwola, D.M., David, O.T., Adeyemo, S.F., Ayodeji, O.D., Akinade, E.M., Saibu, O.A., 2024. Microbial mysteries: Staphylococcus aureus and the enigma of carcinogenesis. Microb Pathog 194, 106831. https://doi.org/10.1016/j.micpath.2024.106831

O'Neill J. Tackling drug-resistant infections globally: final report and recommendations. London: Review on Antimicrobial Resistance, 2016.

Parai, D., Banerjee, M., Dey, P., Mukherjee, S.K., 2020. Reserpine attenuates biofilm formation and virulence of Staphylococcus aureus. Microb Pathog 138, 103790. https://doi.org/10.1016/j.micpath.2019.103790

Qian, W., Liu, M., Fu, Y., Zhang, J., Liu, W., Li, J., Li, X., Li, Y., Wang, T., 2020. Antimicrobial mechanism of luteolin against Staphylococcus aureus and Listeria monocytogenes and its antibiofilm properties. Microb Pathog 142, 104056. https://doi.org/10.1016/j.micpath.2020.104056

Qiao, J., Zheng, L., Lu, Z., Meng, F., Bie, X., 2021. Research on the biofilm formation of staphylococcus aureus after cold stress. Microorganisms 9, 1534. https://doi.org/10.3390/microorganisms9071534

Raduan, S.Z., Ahmed, Q.A., Kasmuri, A.R., Rusmili, M.R.A., Mia, M.A.R., Sulaiman, W.M.A.W., Mahmood, M.H., Shaikh, M.F., 2022. Antioxidant capabilities of Litsea garciae bark extracts and their relation to the phytochemical compositions. Malays Appl Biol 51, 99-118. https://doi.org/10.55230/mabjournal.v51i1.2038

Riyadi, P.H., Susanto, E., Anggo, A.D., Arifin, M.H., Rizki, L., 2023. Effect of methanol solvent concentration on the extraction of bioactive compounds using ultrasonic-assisted extraction (UAE) from Spirulina platensis. Food Res 7, 59-66. https://doi.org/10.26656/fr.2017.7(s3).9

Sarian, M.N., Ahmed, Q.U., Mat So'ad, S.Z., Alhassan, A.M., Murugesu, S., Perumal, V., Syed Mohamad, S.N.A., Khatib, A., Latip, J., 2017. Antioxidant and antidiabetic effects of flavonoids: A structure-activity relationship-based study. BioMed Res Int 2017, 8386065. https://doi.org/10.1155/2017/8386065

Settaluri, V.S., Al Anbari, T.M., Al Shukaili, S.K., Al Rawahi, R.M., Azmi, S.N.H., Sah, P., Reddy, S.H., Ahmed, Q.U., Hussain, S.A., Daddam, J.R., Sah, S., Mahmood, S., 2024. Phytochemical screening and in vitro evaluation of antioxidant and antimicrobial efficacies of Pteropyum scoparium (Jaub. Spach) Sidaf crude extracts. J King Saud Univ Sci 36, 102995. https://doi.org/10.1016/j.jksus.2023.102995

Sitthan, V.K., Abdallah, M.S., Nallappan, M., Choi, S.H., Paik, J.H., Go, R., 2023. Antioxidant and Antibacterial Activity of Different Solvent Extracts of Leaves and Stem of Alyxia reinwardtii Blume. MAB 52, 67-80. https://doi.org/10.55230/mabjournal.v52i6.2581

Tao, X., Wang, H., Min, C., Yu, T., Luo, Y., Li, J., Hu, Y., Yan, Q., Liu, W.E., Zou, M., 2020. A retrospective study on Escherichia coli bacteremia in immunocompromised patients: Microbiological features, clinical characteristics, and risk factors for shock and death. J Clin Lab Anal 34, e23319. https://doi.org/10.1002/jcla.23319

Umar, A., Faidallah, H.M., Ahmed, Q.U., Alamry, K.A., Mukhtar, S., Alsharif, M.A., Azmi, S.N.H., Parveen, H., Zakaria, Z.A., Hussien, M.A., 2022. Design, synthesis, in vitro antiproliferative effect and in situ molecular docking studies of a series of new benzoquinoline derivatives. J King Saud Univ Sci 34, 102003. https://doi.org/10.1016/j.jksus.2022.102003

Veiga, A., Toledo, M.D.G.T., Rossa, L.S., Mengarda, M., Stofella, N.C.F., Oliveira, L.J., Gonçalves, A.G., Murakami, F.S., 2019. Colorimetric microdilution assay: Validation of a standard method for determination of MIC, IC50%, and IC90% of antimicrobial compounds. J Microbiol Methods 162, 50-61. https://doi.org/10.1016/j.mimet.2019.05.003

Wang, Z., Ding, Z., Li, Z., Ding, Y., Jiang, F., Liu, J., 2021. Antioxidant and antibacterial study of 10 flavonoids revealed rutin as a potential antibiofilm agent in Klebsiella pneumoniae strains isolated from hospitalized patients. Microb Pathog 159, 105121. https://doi.org/10.1016/j.micpath.2021.105121

Yu, L., Maishi, N., Akahori, E., Hasebe, A., Takeda, R., Matsuda, A.Y., Hida, Y., Nam, J.M., Onodera, Y., Kitagawa, Y., Hida, K., 2022. The oral bacterium streptococcus mutans promotes tumor metastasis by inducing vascular inflammation. Cancer Sci. 113, 3980-3994. https://doi.org/10.1111/cas.15538

Zhang, Q.W., Lin, L.G., Ye, W.C., 2018. Techniques for extraction and isolation of natural products: A comprehensive review. Chin Med 13, 20. https://doi.org/10.1186/s13020-018-0177-x